Dalton Transactions

ROYAL SOCIETY OF CHEMISTRY

PAPER

View Article Online
View Journal | View Issue

Cite this: *Dalton Trans.*, 2025, **54**, 7793

Reaction of a non-heme iron-nitrosyl with dioxygen: decomposition of the ligand through NOD-like activity†

Riya Ghosh, Rakesh Mazumdar, Bapan Samanta, Shankhadeep Saha and Biplab Mondal *

A high-spin iron(II) nitrosyl, [(TPz)Fe(NO)](ClO$_4$)$_2$, **2** (TPz = Tris(3,5-dimethylpyrazol-1-ylmethyl)amine) with an {Fe(NO)}^{7} configuration was synthesized and characterized structurally. The dioxygen reactivity of complex **2** in acetonitrile solution results in the oxidation of the ligand. Chemical evidence suggests the involvement of a peroxynitrite intermediate in this reaction. A trapping experiment shows the formation of NO_2 during the reaction which supports the proposition of the involvement of the peroxynitrite intermediate. This study gives an insight into an alternate possibility from the dioxygen reactivity of metal-nitrosyl leading to nitric oxide dioxygenase (NOD) activity.

Received 2nd January 2025,
Accepted 6th April 2025

DOI: 10.1039/d5dt00009b

rsc.li/dalton

Introduction

Nitric oxide (NO), being an important molecule in mammalian biology, has attracted huge research activity since its discovery as a signaling molecule.[1–3] The overproduction of NO can be lethal due to the formation of secondary reactive nitrogen species (RNS) such as nitrogen dioxide (NO_2) and peroxynitrite ($OONO^-$).[4,5] The concentration of NO *in vivo* is regulated by the enzymes nitric oxide dioxygenases (NODs). It is known that in NOD activity, the oxy-heme (*i.e.*, iron(III)-superoxo) species of the NODs reacts with NO and forms the biologically benign nitrate (NO_3^-) ion.[6,7] This reaction presumably proceeds through a peroxynitrite intermediate, Fe^{III}-($OONO^-$). It is proposed that an oxo-ferryl, [Fe^{IV}(O)], species formed in the reaction *via* the homolytic cleavage of the O–O bond of the Fe^{III}-($OONO^-$) intermediate (Scheme 1).

Such an oxo-ferryl species has been evidenced spectroscopically in the reaction of myoglobin with $OONO^-$ ions.[8] Although, in the literature, the involvement of a proposed metal-peroxynitrite species was exemplified in the reactions of NO with a metal–oxygen adduct or in the reactions of metal-nitrosyls with reactive oxygen species (O_2, $O_2^{\bullet-}$, O_2^{2-}), direct evidence is still elusive.[9–16] This is because of the very short life time of metal-peroxynitrite. In addition, evidence for the formation of high valent metal-oxo species from the homolytic O–O bond cleavage of the metal-peroxynitrite intermediate is also scarce because of the very fast recombination of the metal-oxo species with NO_2 in the reaction cage to result in NO_3^-.

Peroxynitrite, being a strong oxidizing/nitrating agent, catalyzes the oxidation and/or nitration of various biological substrates like lipid, protein (specifically tyrosine) *etc*. The tyrosine nitration by peroxynitrite is, in fact, used as a marker for NO metabolism in biological systems. In small molecule model studies, the existence of a short-lived peroxynitrite intermediate is authenticated using this tyrosine (phenol ring) nitration test. However, in no case with a heme group, the nitration of the porphyrin ring has been reported.[12,14–16c–e] Similarly, the

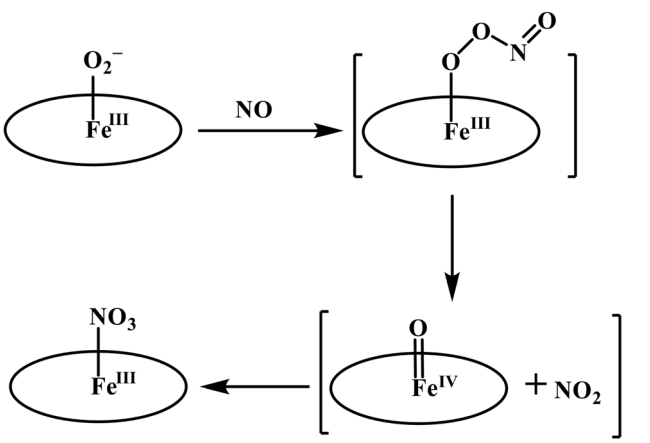

Scheme 1

Department of Chemistry, Indian Institute of Technology Guwahati, Assam – 781039, India. E-mail: biplab@iitg.ac.in; Fax: (+)91-361-258-2339; Tel: (+)91-361-258-2317

† Electronic supplementary information (ESI) available: Spectral analyses, crystallographic data and metric parameters of the complexes. CCDC 2170068, 2170069, 2170070, and 2170071. For ESI and crystallographic data in CIF or other electronic format see DOI: https://doi.org/10.1039/d5dt00009b

oxidation/nitration of the ligand framework is also not known in the reaction of non-heme models where a putative peroxynitrite is presumed. As such, no metal nitrosyl is known which, by itself, undergoes ring/ligand nitration/oxidation in the presence of dioxygen.

Herein, we report the dioxygen reactivity of a non-heme iron-nitrosyl complex which presumably results in the formation of a metal peroxynitrite intermediate. This has been authenticated by the characteristic ring nitration of the externally added phenolic substrate. In the absence of the phenolic substrate, ligand modification has been observed which is a rare event in the chemistry of dioxygen reactivity of metal nitrosyl. A trapping experiment suggests the formation of NO_2 in the reaction which is expected from the decomposition of a metal-peroxynitrite intermediate (Scheme 1).

Results and discussion

Ligand TPz (TPz = Tris(3,5-dimethylpyrazol-1-ylmethyl)amine) was synthesized following an earlier report (Experimental section; ESI, Fig. S1–S7†).[17] The metal complex, $[Fe^{II}(TPz)(CH_3CN)(H_2O)](ClO_4)_2$, **1** was prepared by stirring an equimolar mixture of TPz and $[Fe^{II}(CH_3CN)_4(ClO_4)_2]$ in dry acetonitrile under an Ar atmosphere (Experimental section). The precursor complex **1** was characterized spectroscopically and by its X-ray single crystal structure determination (ESI, Fig. S8–S12†). Addition of NO gas to the dry and degassed acetonitrile solution of complex **1** leads to the formation of the green colored complex **2**, $[Fe(TPz)(NO)(CH_3CN)](ClO_4)_2$ (Experimental section). Complex **2** having $\{Fe(NO)\}^7$ configuration was isolated as a solid and structurally characterized (ESI, Fig. S13–S15†). The ORTEP diagram of complex **2** is shown in Fig. 1. The crystal structure shows that the iron center is coordinated with four N atoms from the TPz ligand, one acetonitrile, and one NO group in a distorted octahedral geometry. It would be worth mentioning here that analogous nitrosyl complexes of Fe with the same ligand framework, $[(TPz)Fe(NO)(OClO_3)]^+$ and $[(TPz)Fe(NO)(Cl)]^+$, were reported earlier.[18] In both the cases, the iron center was coordinated with a counter anion along with the ligand and NO group.

In complex **2**, the Fe–N_{NO} distance is 1.732 Å. The N–O distance and Fe–N–O bond angle are 1.132 Å and 174.2°, respectively. The parameters are slightly different from those of the perchlorate anion coordinated nitrosyl complexes reported earlier (Table 1).[18] For instance, in complexes $[(TPz)Fe(NO)(OClO_3)]^+$/$[(TPz)Fe(NO)(Cl)]^+$ the Fe–N_{NO} distance is 1.767/1.735 Å, the N–O distance is 1.103/1.15 Å and the Fe–N–O angle is 162.5°/157.1°.[18] In $[Fe(TPA)(NO)(BenzFor)]^+$ (BenzFor = benzoylformate), the Fe–N_{NO} distance is 1.70 Å, the N–O distance is 1.15 Å and the Fe–N–O angle is 162°.[19a] It is evident that Fe–N–O is more linear in the case of complex **2** than those reported earlier. The nitrosyl stretching frequency for complex **2** appeared at 1790 cm^{-1} (ESI, Fig. S13†) which matches well with the reported ones.[18,19] The X-band EPR spectrum of complex **2** displays two sets of signals at $g \sim 4.11$ and 2.04 corresponding to the near axial high spin ($s = 3/2$) iron(II) nitrosyl (ESI Fig. S15†).[20] The sharp isotropic signal near $g = 2$ is

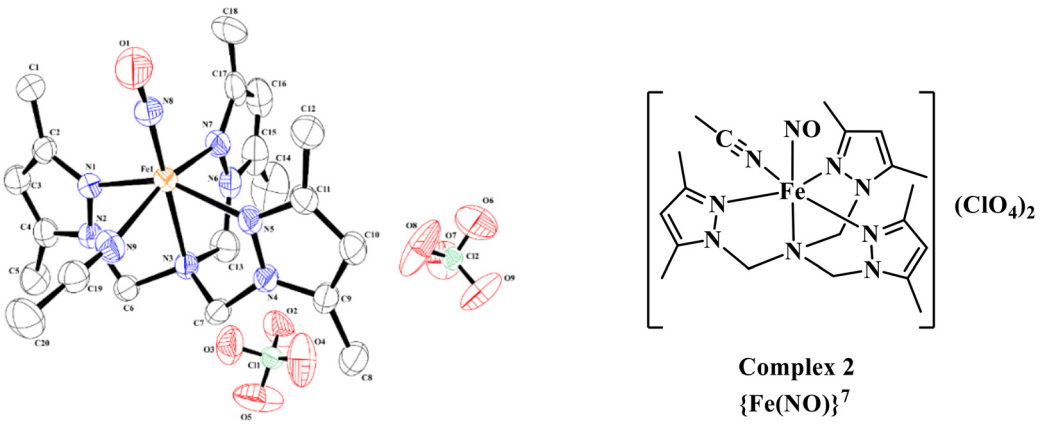

Fig. 1 ORTEP diagram of complex **2** (30% thermal ellipsoid plot, H atoms are omitted for clarity).

Table 1 List of bond lengths, angles and stretching frequency for reported analogous iron-nitrosyls

Compound	Fe–N_{NO} length (Å)	N–O length (Å)	Fe–N–O angle (°)	ν(NO) in cm^{-1}	Ref.
$[(TPz)Fe(NO)(OClO_3)]^+$	1.767	1.103	162.5	—	18*b*
$[(TPz)Fe(NO)(Cl)]^+$	1.735	1.15	157.1	1796	18*b*
$[Fe(TPA)(NO)(BenzFor)]^+$	1.722	1.152	159.2	1794	19*a*
$[Fe(TPA)(NO)(OTf)](OTf)$	1.755	1.144	170	1806	19*b*
$[Fe(TPz)(NO)(CH_3CN)]^{2+}$	1.732	1.132	174.2	1790	This work

perhaps due to the presence of a very small amount of $S = \frac{1}{2}$ impurity. In the cases of $[Fe(TPA)(NO)(BenzFor)]^+$ and $[Fe(^6TLA)(NO)(BenzFor)]^+$ these resonances appear at g = 4.05, 3.87, 1.99 and g = 4.02, 3.93, 1.95, respectively.[19]

Dioxygen reactivity of complex 2

In the UV-visible spectrum, complex **2** exhibited characteristic absorption bands at 610 nm (ε/M^{-1} cm^{-1}, 586), 351 nm (ε/M^{-1} cm^{-1}, 4899) and 249 nm (ε/M^{-1} cm^{-1} 20833). The addition of O_2 gas to the degassed acetonitrile solution of complex **2** at room temperature resulted in the increase of the intensity of the 351 nm band with a simultaneous decrease of the intensity of the 610 nm band with respect to time and resulted in the final product within 5 minutes (Fig. 2). The final product was isolated as a solid and characterized spectroscopically as the corresponding nitrate complex, **3** (ESI, Fig. S17–S19†). The 1384 cm^{-1} band in the FT-IR spectrum of complex **3** suggested the presence of a nitrate (NO_3^-) group (ESI, Fig. S17†).[21]

In FT-IR spectroscopic monitoring, addition of O_2 gas into the degassed acetonitrile solution of complex **2** resulted in the disappearance of the NO stretching frequency at 1799 cm^{-1} while a new band appeared at 1835 cm^{-1} simultaneously (Fig. 3).

The intensity of this stretching frequency was found to decay with time and finally disappeared, suggesting the formation of an unstable intermediate. Fe(II) complexes in both the heme and non-heme frameworks are known to react with O_2 leading to the formation of the corresponding $[Fe^{III}(O_2^-)]$ species where the metal center is oxidized by one unit.[7b] In general, metal-superoxide type adducts exhibit $\nu(O_2)$ in the range of 1200–1070 cm^{-1} and metal-peroxo adducts display O–O stretching in the range of 930–740 cm^{-1}.[22,23] However, no such characteristic stretching was observed in this case except for a weak stretching at 1018 cm^{-1}. This 1018 cm^{-1} is a bit lower for a metal-superoxide and in the higher side for metal-peroxo adducts. In addition, when the reaction was carried out with $^{18}O_2$, the NO stretching frequency was found to shift to 1835 cm^{-1}, as expected, but no change was observed for the stretching at 1018 cm^{-1}, suggesting its non-O–O nature. On the other hand, in the literature, the nitrosyl stretching frequency in $\{Fe(NO)\}^6$ is reported to appear at ~1830 cm^{-1}.[24] Thus, the 1835 cm^{-1} band can be attributed to the nitrosyl stretching of the $\{Fe(NO)\}^6$ moiety which is formed upon the reaction of $\{Fe(NO)\}^7$ with O_2. This was further confirmed by the ^{15}NO labelling experiment where the band was found to appear at 1801 cm^{-1}. It would be worth mentioning here that the structurally characterized non-heme $\{Fe(NO)\}^6$ complex, $[Fe(TMG_3tren)(NO)]^{3+}$, displays nitrosyl stretching at 1879 cm^{-1}.[24b] Spectroscopic and theoretical studies suggest that the electronic structure can be best explained by a high-spin Fe(IV) coordinated to a triplet NO^- unit.[24b] Considering the spectral evidence, it is logical to assume that the reaction of complex **2** with O_2 results in the formation of $[Fe^{III}(NO)]^{3+}$ and O_2^- which are present in the reaction cage, but the O_2^- is not coordinated to the metal center (Scheme 2).

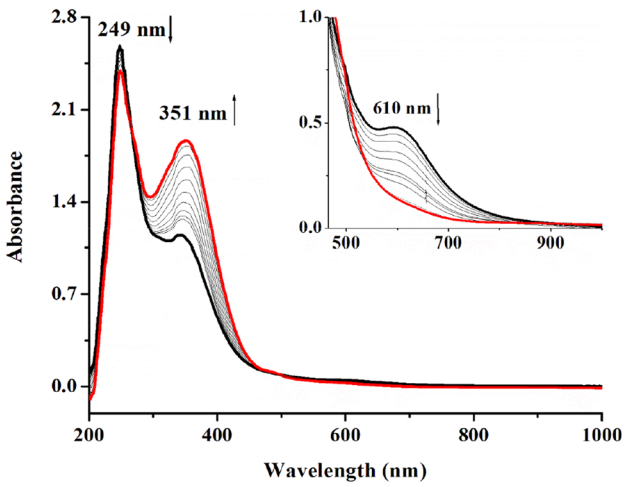

Fig. 2 UV-visible spectra of the reaction of complex **2** (thick black trace) with O_2 and formation of complex **3** (red trace) [inset: complex **2** (black), after O_2 addition] in acetonitrile at room temperature.

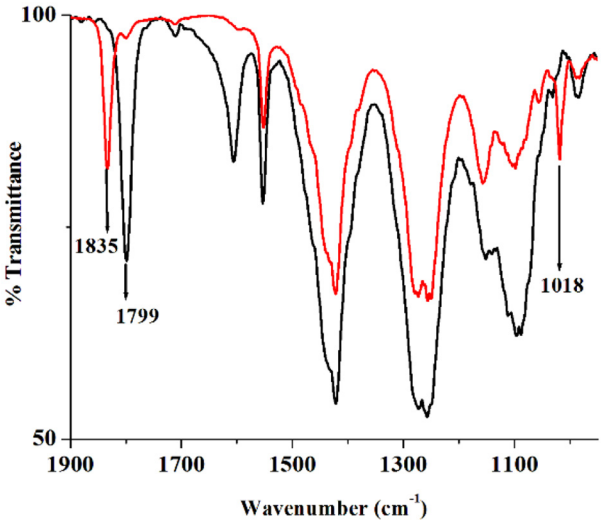

Fig. 3 FT-IR spectra of the reaction of complex **2** with O_2 in acetonitrile medium [complex **2** (black), after O_2 addition (red)].

When the reaction was carried out at −40 °C the same spectral changes were observed in UV-visible and FT-IR spectroscopic studies. Upon keeping the reaction mixture in a freezer for 2 days, white crystals of the modified ligand (**L′**) and a brown precipitate of complex **4**, $[Fe(OH)_3]$ (isolated in polymeric form), were obtained. They were characterized using various spectroscopic methods (Experimental section; ESI, Fig. S20–S26†) and by single crystal structure determination. The perspective ORTEP view of **L′** is shown in Fig. 4.

Interestingly, when the reaction mixture was warmed up to room temperature quickly, $[(TPz)Fe^{III}(NO_3)](ClO_4)_2$, complex **3**, was obtained as a final product.

NO and O_2^- ions are believed to react to result in a peroxynitrite ($OONO^-$) intermediate. We propose that the reaction of complex **2** with O_2 leads to the initial formation of {[(TPz)

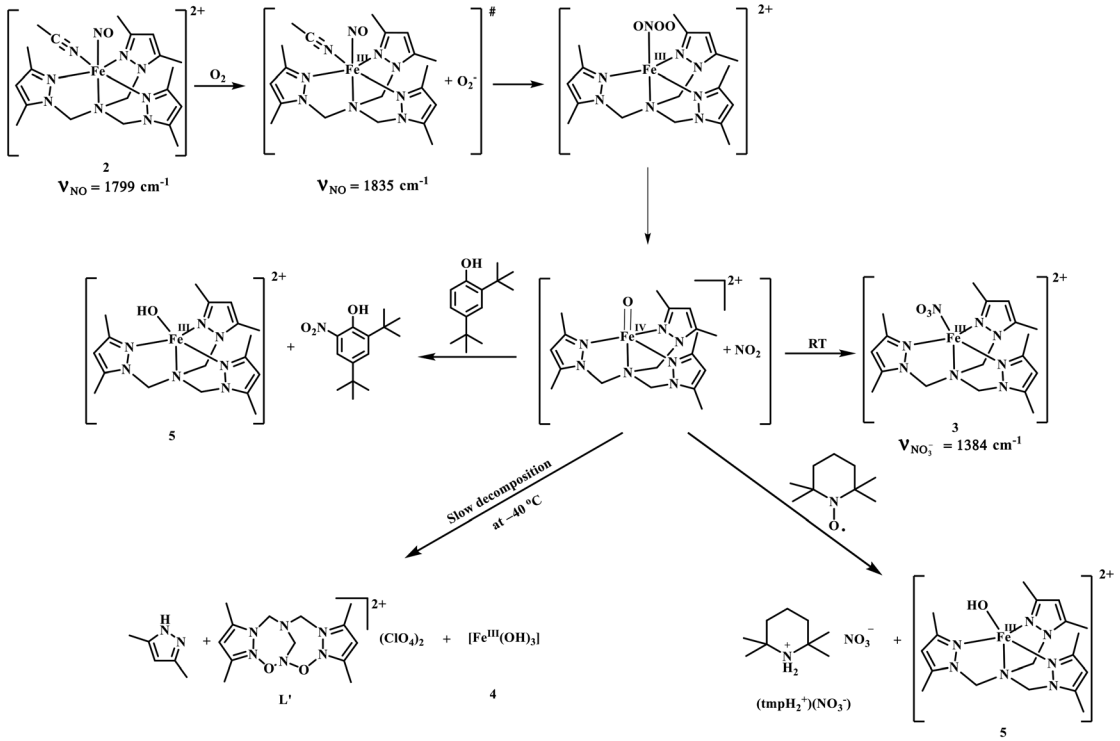

Scheme 2 Overall reaction.

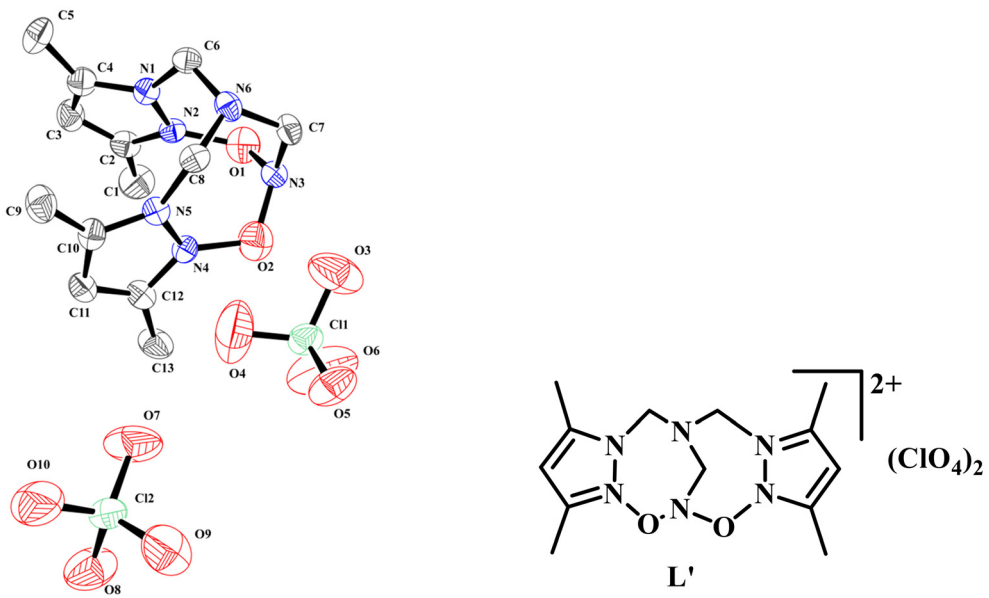

Fig. 4 ORTEP diagram of the modified ligand (L′) (30% thermal ellipsoid plot, H atoms are omitted for clarity).

$Fe^{III}(NO)]^{3+}\cdot(O_2^{-})\}$ in the reaction cage as an intermediate which subsequently forms the corresponding peroxynitrite intermediate $[(TPz)Fe^{III}(OONO^{-})]^{2+}$ (Scheme 2). The peroxynitrite intermediate decomposes leading to the corresponding oxo-ferryl, $[(TPz)Fe^{IV}(O)]^{2+}$ species and NO_2. They recombine very fast in a quick warm up process and result in complex **3**. However, when the reaction mixture was kept in the freezer for a couple of days, **L′** was formed.

It was reported earlier that the methylene group in a pyrazolyl moiety, in the presence of a radical initiator, results in the corresponding radical.[25] In the present case, $[(TPz)Fe^{IV}(O)]^{2+}$ abstracts a H$^{\cdot}$ from the methylene carbon of the pyrazolyl

group and the corresponding radical is formed. This radical then reacts with NO_2 resulting in **L′**. To support this finding, a few control experiments have been carried out. When 2,4-ditertiarybutylphenol was added in the reaction mixture as external substrate, 2,4-ditertiarybutyl-6-nitrophenol (*ca.* 65%) was obtained along with $[(TPz)Fe^{III}(OH)]^{2+}$, **5** (Experimental section; ESI, Fig. S27–S32†). This is because, in the presence of an external electron rich phenolic substrate, the oxo-ferryl moiety reacts with the substrate to form a phenoxyl radical and $[(TPz)Fe^{III}(OH)]^{2+}$, **5**. The phenoxyl radical then combines with NO_2 to afford the nitrophenol product (Scheme 2), as expected. This experiment, in turn, supports the proposition of the formation of a peroxynitrite intermediate. If the reaction proceeds through a pathway as proposed in Scheme 2, the presence of a substrate which can react with NO_2 is expected to inhibit the formation of **L′**. When the reaction was carried out in the presence of TEMPO, the formation of **L′** was not observed. Complex **5** and 2,2,6,6-tetramethylpiperidin-1-ium nitrate $(\mathbf{tmpH_2^+})(\mathbf{NO_3^-})$ were isolated from the reaction mixture. Spectroscopic characterization and single crystal X-ray structure determination confirm the formulation of $(\mathbf{tmpH_2^+})(\mathbf{NO_3^-})$ (Experimental section; ESI, Fig. S33 and S34†). The ORTEP diagram is shown in Fig. 5.

Thus, while we do not have any spectroscopic evidence for the formation of the peroxynitrite intermediate, based on the control experiments, the formation of a peroxynitrite intermediate in the reaction is presumed.

Experimental section

Materials and methods

All chemicals and solvents were of commercially available quality and used without further purification, unless otherwise mentioned. Anhydrous $[Fe^{II}(CH_3CN)_4(ClO_4)_2]$ was prepared using a previously reported procedure.[26] Acetonitrile was distilled over phosphorus pentoxide under Ar. Diethyl ether was distilled with sodium metal and benzophenone. All the dry solvents were stored over 4 Å molecular sieves under inert conditions. Deoxygenation of the solvent and solutions was effected by repeated vacuum/Ar purge cycles or bubbling with Ar for 30 min. All the reactions were performed under inert conditions unless specified. UV-visible spectra were recorded on an Agilent Technologies Cary 8454 UV-visible spectrophotometer by preparing a known concentration of the samples in acetonitrile solution at room temperature (25 °C) using a quartz cuvette of 1 cm width. FT-IR spectra of the samples were taken on a PerkinElmer spectrophotometer at room temperature with samples prepared either as KBr pellets by grinding the sample with KBr (IR-grade) or in acetonitrile solution in a KBr cell. ^{1}H and ^{13}C NMR spectra were collected in 400 MHz Bruker AVANCE 400 and 500 MHz Bruker AVANCE NEO 500 FT-NMR spectrometers. Chemical shifts were reported as δ (ppm) values relative to an internal standard (tetramethylsilane) and the residual solvent peaks. The X-band electron paramagnetic resonance (EPR) spectra were recorded on a JEOL JES-FA200 ESR spectrometer, at 77 K with a microwave power of 0.998 mW and a microwave frequency of 9.14 GHz. Mass spectra were measured in HPLC grade acetonitrile solution.

Single crystals of all complexes suitable for X-ray crystallographic analysis were obtained by layering of diethyl ether into the acetonitrile solution. The intensity data were collected using a Bruker SMART APEX-II CCD diffractometer, equipped with fine focus 1.75 kW sealed tube MoK_α radiation (λ = 0.71073 Å) at 293(3) K, with increasing ω (width of 0.3° per frame) at a scan speed of 3 s per frame. The SMART software was used for data acquisition. Data integration and reduction were undertaken with SAINT and XPREP software.[27] Multi-scan empirical absorption corrections were employed to the data using the program SADABS.[28] Structures were solved by direct methods using SHELXS-2016 and refined with full-matrix least squares on F^2 using SHELXL-2016/6.[29] Structural illustrations have been drawn with ORTEP-3 for Windows.[30]

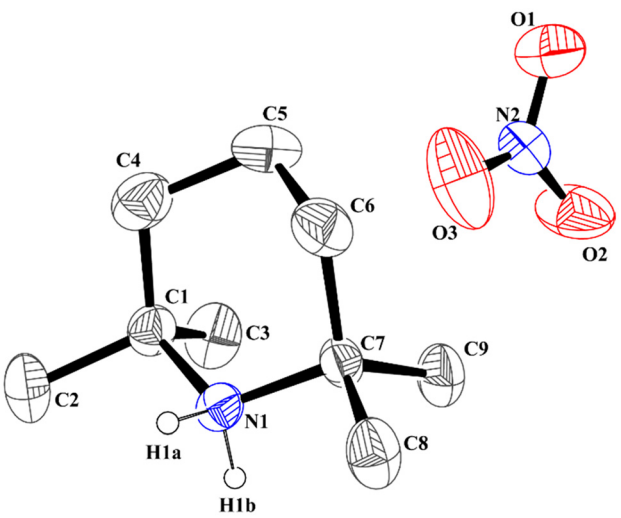

Fig. 5 ORTEP diagram of $(\mathbf{tmpH_2^+})(\mathbf{NO_3^-})$ (30% thermal ellipsoid plot, H-atoms are omitted for clarity).

Syntheses

Tris(3,5-dimethylpyrazol-1-ylmethyl)amine, TPz. The ligand TPz was synthesized following a previously reported procedure.[17] Elemental analyses of $C_{18}H_{27}N_7$, calcd (%): C, 63.32; H, 7.97; N, 28.71, found (%): C, 63.56; H, 7.81; N, 28.34. FT-IR (in KBr): 2922, 1555, 1461, 1313, 1186, 1103, 1029 and 779 cm^{-1}. ^{1}H NMR (400 MHz, $CDCl_3$): δ_{ppm}, 5.76 (s, 3H), 4.96 (s, 6H), 2.18 (s, 9H), 1.82 (s, 9H); ^{13}C NMR (100 MHz, $CDCl_3$): δ_{ppm}, 147.6, 140.1, 105.9, 62.4, 13.3, 9.9. ESI-mass (m/z): calcd: 341.46, found: 342.24 (M + 1), 364.23 (M + Na)$^+$.

$[Fe^{II}(TPz)(CH_3CN)(H_2O)](ClO_4)_2$, 1. $[Fe(CH_3CN)_4(ClO_4)_2]$ (0.210 g, 0.5 mmol) was dissolved in dry and degassed acetonitrile.[26] The solution of the ligand TPz (0.170 g, 0.5 mmol) in acetonitrile medium was also degassed under an Ar atmosphere. After that, two solutions were mixed and the color of the solution became pale yellow. The solution was stirred for

30 minutes under an argon atmosphere. After that the solution was layered with diethyl ether and kept in a refrigerator. After 1day a white crystalline precipitate of complex **1** was formed with ~62% yield (0.21 g). Elemental analyses of $C_{20}H_{32}N_8O_9Cl_2Fe$, calcd (%): C, 52.64; H, 7.07; N, 24.55, found (%): C, 52.35; H, 7.28; N, 24.82. FT-IR (in KBr): 1637, 1555, 1464, 1423, 1395, 1313, 1274, 1145, 1117, 1084, 886, 806, 636 and 626 cm^{-1}. UV-visible (CH_3CN) 836 nm (ε/M^{-1} cm^{-1}, 462) and 328 nm (ε/M^{-1} cm^{-1}, 4850). ESI-mass (m/z): calcd: 198.58, found: 198.61 for $[FeTPz]^{2+}$.

$[Fe^{II}(TPz)(NO)(CH_3CN)](ClO_4)_2$, 2. Complex **1** (0.65 g, 1 mmol) was dissolved in 10 mL dry and degassed acetonitrile. To this solution NO gas was purged for 3 minutes until the color changed to dark green. The next day excess NO gas was removed by applying several cycles of vacuum/Ar purged. Then the solution was layered with diethyl ether and after a few days green crystals of complex **2** were obtained. The same procedure has been used to prepare the 15-nitrogen labelled complex **2**. Yield: 0.48 g (~73%). Elemental analysis of $C_{20}H_{30}N_9O_9Cl_2Fe$, calcd (%): C, 36.00; H, 4.53; N, 18.89, found (%): C, 36.35; H, 4.20; N, 18.09. FT-IR (in KBr): 1789, 1617, 1554, 1465, 1421, 1391, 1313, 1274, 1248, 1140, 1113, 1088, 940, 887, 805 and 626 cm^{-1}; FT-IR in CH_3CN, ν_{NO} = 1799 cm^{-1} {for ^{15}NO, 1765 cm^{-1}}. UV-visible (CH_3CN): 610 nm (ε/M^{-1} cm^{-1}, 586), 351 nm (ε/M^{-1} cm^{-1}, 4899) and 249 nm (ε/M^{-1} cm^{-1}, 20833).

Reaction of complex 2 with O_2. Complex **2** (0.66 g, 1 mmol) was dissolved in 5 mL of dry and degassed acetonitrile. To this solution O_2 gas was bubbled for 2 minutes. After some time, the color of the solution changes from green to brown. This brown colored solution was immediately precipitated out after being layered with ether and isolated as a solid of complex $[Fe^{III}(TPz)(NO_3)](ClO_4)_2$, **3**. The reaction of complex **2** with O_2 was monitored by solution phase FT-IR, UV-visible and EPR spectroscopy.

Complex 3. Yield: 0.49 g (~75%). FT-IR (in KBr):1632, 1556, 1466, 1422, 1384, 1309, 1252, 1144, 1119, 1087, 833, 636 cm^{-1}. UV-visible (CH_3CN): 359 nm (ε/M^{-1} cm^{-1}, 6288), 910 nm (ε/M^{-1} cm^{-1}, 198). ESI-mass (m/z) ($[Fe^{III}(TPz)(NO_3)(ClO_4)]^+$ unit): calcd: 558.104; found: 558.289.

$Fe^{III}(OH)_3$ (polymeric form), 4 and modified ligand (L′). The brown colored solution obtained from the reaction of complex **2** (0.66 g, 1 mmol) with O_2 was layered with diethyl ether and kept in the refrigerator. After that white crystals of the modified ligand (**L′**) was obtained along with complex **4**.

Complex 4. Yield: 0.06 g (~60%). FT-IR (in KBr): 1633, 1557, 1423, 1253, 1144, 1121, 1084 and 626 cm^{-1}. UV-visible (CH_3CN): 345 nm (ε/M^{-1} cm^{-1}, 8452), 910 nm (ε/M^{-1} cm^{-1}, 198).

Modified ligand (L′). Yield: 0.32 g (~65%). FT-IR (in KBr): 1655, 1557, 1456, 1426, 1385, 1368, 1338, 1264, 1252, 1152, 1116, 1083, 1040, 995, 918, 829, 735, 678, 626 cm^{-1}. ^{1}H-NMR (400 MHz, $CDCl_3$): δ_{ppm}: 5.78 (s, 2H), 5.29 (s, 2H), 4.98 (s, 4H), 2.20 (s, 6H), 1.84 (s, 6H).^{13}C NMR (100 MHz, CD_3CN) δ_{ppm}, 207.7, 149.1, 110.3, 78.1, 68.2, 31, 12.8.

$[Fe^{III}(TPz)(OH)](ClO_4)_2$, 5 and 2,4-di-*tert*-butyl-6-nitrophenol. To the dry and degassed acetonitrile solution of complex **2** (0.66 g, 1 mmol), degassed solution of 2,4-di-*tert*-butylphenol (0.51 g, 5 mmol) in acetonitrile was added followed by the addition of O_2 gas at room temperature. The reaction mixture was washed with hexane several times. 2,4-Di-*tert*-butyl-6-nitrophenol was separated by preparative TLC of the hexane solution and complex **5** was obtained from the acetonitrile part of the reaction mixture.

Complex 5. Yield: 0.45 g (~73%). FT-IR (in KBr): 1633, 1555, 1465, 1423, 1384, 1260, 1275, 1141, 1120, 1088 and 627 cm^{-1}. UV-visible (CH_3CN): 915 nm (ε/M^{-1} cm^{-1}, 315); 320 nm (ε/M^{-1} cm^{-1}, 7208). ESI-mass (m + 1)/z: calcd: 613.075, found: 613.176.

2,4-Di-*tert*-butyl-6-nitrophenol. Yield: 0.16 g (~65%). ^{1}H NMR (400 MHz, $CDCl_3$): δ_{ppm}, 11.44 (s, 1H), 7.96 (s, 1H), 7.65 (s, 1H), 1.45 (s, 9H), 1.32 (s, 9H). ^{13}C NMR (100 MHz, $CDCl_3$): δ_{ppm}, 153.0, 142.0, 139.9, 133.7, 132.5, 118.9, 35.7, 34.5, 31.1, 29.4. ESI-mass (m/z): calcd: 251.15, found: 250.23 (M − 1).

Reaction of complex 2 with O_2 and 2,2,6,6-tetramethylpiperidin-1-yloxyl (TEMPO). Complex **2** (0.66 g, 1 mmol) and TEMPO (0.8 g, 5 mmol) were dissolved in 10 mL dry and degassed acetonitrile solution followed by the addition of O_2. After completion the reaction mixture was extracted with hexane solution. The hexane part contains 2,2,6,6-tetramethylpiperidin-1-ium nitrate **$(tmpH_2^+)(NO_3^-)$** and unreacted TEMPO, whereas the acetonitrile part contains complex **5**.

2,2,6,6-Tetramethylpiperidin-1-ium nitrate $(tmpH_2^+)(NO_3^-)$. Yield: 0.76 g (~60%).^{1}H NMR (500 MHz, $CDCl_3$): δ_{ppm}, 1.74 (s, 6H), 1.48 (s, 12H). ^{13}C NMR (125 MHz, $CDCl_3$): δ_{ppm}, 56.8, 35.0, 27.5, 16.3.

Reaction of complex 2 with $Ag^I(ClO_4)$. Complex **2** (0.33 g, 0.5 mmol) was dissolved in 3 mL dry and degassed acetonitrile. $Ag^I(ClO_4)$ (0.153 g, 0.75 mmol) was dissolved in 0.01 mL dry and degassed acetonitrile and added to the solution of complex **2** resulting in the formation of the corresponding $\{Fe(NO)\}^6$ intermediate. In FT-IR studies, the nitrosyl stretching frequency at 1799 cm^{-1} was shifted to 1835 cm^{-1} suggesting the oxidation of complex **2**.

Conclusion

Thus, the high spin Fe(II)-nitrosyl, [(TPz)Fe(NO)], having an $\{Fe(NO)\}^7$ configuration in acetonitrile solution was found to react with O_2 to result in the ligand modification to **L′** through a presumed peroxynitrite intermediate. In contrast, heme $\{Fe(NO)\}^7$ complexes are known to react with O_2 leading to the formation of the corresponding nitrate (NO_3^-) complexes; but no reports are known where the ligand modification takes place. Although there is no spectroscopic evidence of the formation of the peroxynitrite intermediate, characteristic phenol ring nitration supports the proposition. Additionally, the trapping of NO_2 formed in the reaction also is in agreement with the proposed mechanism. This study, thus, gives an insight into the mechanism of the reaction of metal-nitrosyls with dioxygen leading to the NOD activity.

Crystal data

Complex 1

CCDC 2170069.† $C_{20}H_{34}Cl_2N_8O_{10}Fe$, M = 673.30, triclinic ($P\bar{1}$), a = 11.9018(6), b = 11.9774(6), c = 12.2326(6) Å, α = 84.555(3)°, β = 74.331(3)°, γ = 68.652(2)°, V = 1563.78(14) Å^3, Z = 2, D_c = 1.430 g cm^{-3}, μ = 0.714 mm^{-1}, T = 296(2) K, 5502 reflections, 4355 independent, $R(F)$ = 0.0564 [$I > 2\sigma(I)$], R(int) = 0.0723, w$R(F^2)$ = 0.1771 (all data), GOF = 1.012.

Complex 2

CCDC 2170071.† $C_{20}H_{30}Cl_2N_9O_9Fe$, M = 667.28, monoclinic ($P21/n$), a = 10.4501(6), b = 19.7521(12), c = 15.8247(9) Å, α = 90°, β = 91.422(4)°, γ = 90°, V = 3265.4(3) Å^3, Z = 4, D_c = 1.357 g cm^{-3}, μ = 0.682 mm^{-1}, T = 101(2) K, 5764 reflections, 3822 independent, $R(F)$ = 0.0770 [$I > 2\sigma(I)$], R(int) = 0.1158, w$R(F^2)$ = 0.2159 (all data), GOF = 1.024.

L′

CCDC 2170068.† $C_{15}H_{23}Cl_2N_7O_{10}$, M = 532.30, monoclinic ($P21$), a = 8.3825(5), b = 9.5056(5), c = 15.3798(8) Å, α = 90°, β = 94.911(5)°, γ = 90°, V = 1220.97(12) Å^3, Z = 2, D_c = 1.448 g cm^{-3}, μ = 0.328 mm^{-1}, T = 293(2) K, 3475 reflections, 2853 independent, $R(F)$ = 0.0641 [$I > 2\sigma(I)$], R(int) = 0.0780, w$R(F^2)$ = 0.1869 (all data), GOF = 1.026.

($tmpH_2^+$)(NO_3^-)

CCDC 2170070.† $C_9H_{18}N_2O_3$, M = 204.27, orthorhombic ($Pca21$), a = 15.56(4), b = 9.90(2), c = 15.75(4) Å, α = 90°, β = 90°, γ = 90°, V = 2426(10) Å^3, Z = 8, D_c = 1.118 g cm^{-3}, μ = 0.083 mm^{-1}, T = 293(2) K, 4258 reflections, 2392 independent, $R(F)$ = 0.0725 [$I > 2\sigma(I)$], R(int) = 0.1360, w$R(F^2)$ = 0.2241 (all data), GOF = 1.023.

Data availability

All the experimental and spectroscopic data related to this manuscript are available in the form of the ESI submitted with the manuscript.†

The crystal data are available from the Cambridge Crystallographic Data Center (**https://www.ccdc.cam.ac.uk/**) using the respective CCDC number.

Conflicts of interest

The authors declare no competing financial interest.

Acknowledgements

The authors would like to thank the Department of Science and Technology, India, for financial support (CRG/2020/001636); RG sincerely thanks DST-INSPIRE (IF-180786) for the scholarship. The authors thank DST-FIST for single crystal X-ray diffraction facility. They also extend their sincere thanks to the Department of Chemistry and CIF, IIT Guwahati, for instrumental facilities. They sincerely thank Dr Pankaj Kumar Koli, IISER Tirupati, India, for providing $Na^{15}NO_2$ generously.

References

1 L. J. Ignarro, *Nitric Oxide: Biology and Pathobiology*, Academic Press, San Diego, 2000.
2 (*a*) S. Moncada, R. M. Palmer and E. A. Higgs, *Pharmacol. Rev.*, 1991, **43**, 109; (*b*) A. R. Butler; and D. L. H. Williams, *Chem. Soc. Rev.*, 1993, **22**, 233; (*c*) *Methods in nitric oxide research*, ed. M. Feelisch and J. S. Stamler, John Wiley and Sons, Chichester, England, 1996; (*d*) L. Jia, C. Bonaventura, J. Bonaventura; and J. S. Stamler, *Nature*, 1996, **380**, 221; (*e*) M. T. Gladwin, J. R. Lancaster Jr., B. A. Freeman and A. N. Schechter, *Nat. Med.*, 2003, **9**, 496.
3 (*a*) M. A. Marletta, P. S. Yoon, R. Iyengar, C. D. Leaf and J. S. Wishnok, *Biochemistry*, 1988, **27**, 8706; (*b*) B. A. Averill, *Chem. Rev.*, 1996, **96**, 2951.
4 (*a*) R. Radi, *Proc. Natl. Acad. Sci. U. S. A.*, 2004, **101**, 4003; (*b*) L. Qiao, Y. Lu, B. Liu and H. H. Girault, *J. Am. Chem. Soc.*, 2011, **133**, 19823; (*c*) N. G. Tran, H. Kalyvas, K. M. Skodje, T. Hayashi, P. Moënne-Loccoz, P. E. Callan, J. Shearer, L. J. Kirschenbaum and E. Kim, *J. Am. Chem. Soc.*, 2011, **133**, 1184.
5 (*a*) S. Goldstein, J. Lind and G. Merenyi, *Chem. Rev.*, 2005, **105**, 2457; (*b*) P. Pacher, J. S. Beckman and L. Liaudet, *Physiol. Rev.*, 2007, **87**, 315; (*c*) A. L. Speelman and N. Lehnert, *Acc. Chem. Res.*, 2014, **47**, 1106.
6 (*a*) M. P. Doyle and J. W. Hoekstra, *J. Inorg. Biochem.*, 1981, **14**, 351; (*b*) C. E. Cooper, J. Torres, M. A. Sharpe and M. T. Wilson, *FEBS Lett.*, 1997, **414**, 281.
7 (*a*) P. R. Gardner, A. M. Gardner, L. A. Martin and A. L. Salzman, *Proc. Natl. Acad. Sci. U. S. A.*, 1998, **95**, 10378; (*b*) M. P. Schopfer, B. Mondal, D.-H. Lee, A. A. N. Sarjeant and K. D. Karlin, *J. Am. Chem. Soc.*, 2009, **131**, 11304; (*c*) N. Lehnert, E. Kim, H. T. Dong, J. B. Harland, A. P. Hunt, E. C. Manickas, K. M. Oakley, J. Pham, G. C. Reed and V. S. Alfaro, *Chem. Rev.*, 2021, **121**, 14682.
8 J. Su and J. T. Groves, *Inorg. Chem.*, 2010, **49**, 6317.
9 P. K. Wick, R. Kissner and W. H. Koppenol, *Helv. Chim. Acta*, 2000, **83**, 748.
10 (*a*) F. Roncaroli, M. Videla, L. D. Slep and J. A. Olabe, *Coord. Chem. Rev.*, 2007, **251**, 1903; (*b*) D. Maiti, D.-H. Lee, A. A. N. Sarjeant, M. Y. M. Pau, E. I. Solomon, K. Gaoutchenova, J. Sundermeyer and K. D. Karlin, *J. Am. Chem. Soc.*, 2008, **130**, 6700.
11 (*a*) T. S. Kurtikyan and P. C. Ford, *Chem. Commun.*, 2010, **46**, 8570; (*b*) T. S. Kurtikyan, S. R. Eksuzyan, J. A. Goodwin and G. S. Hovhannisyan, *Inorg. Chem.*, 2013, **52**, 12046.
12 (*a*) A. Yokoyama, J. E. Han, J. Cho, M. Kubo, T. Ogura, M. A. Siegler, K. D. Karlin and W. Nam, *J. Am. Chem. Soc.*, 2012, **134**, 15269; (*b*) A. Yokoyama, K.-B. Cho, K. D. Karlin and W. Nam, *J. Am. Chem. Soc.*, 2013, **135**, 14900.

13 (*a*) S. G. Clarkson and F. Basolo, *J. Chem. Soc., Chem. Commun.*, 1972, **119**, 670; (*b*) S. G. Clarkson and F. Basolo, *Inorg. Chem.*, 1973, **12**, 1528.
14 K. M. Skodje, P. G. Williard and E. Kim, *Dalton Trans.*, 2012, **41**, 7849.
15 G. Y. Park, S. Deepalatha, S. C. Puiu, D.-H. Lee, B. Mondal, A. A. N. Sarjeant, D. del Rio, M. Y. Pau, E. I. Solomon and K. D. Karlin, *J. Biol. Inorg. Chem.*, 2009, **14**, 1301.
16 (*a*) A. Kalita, P. Kumar and B. Mondal, *Chem. Commun.*, 2012, **48**, 4636; (*b*) S. Saha, S. Ghosh, K. Gogoi, H. Deka, B. Mondal and B. Mondal, *Inorg. Chem.*, 2017, **56**, 10932; (*c*) R. Mazumdar, S. Saha, B. Samanta, R. Ghosh, S. Maity and B. Mondal, *Dalton Trans.*, 2023, **52**, 7917; (*d*) B. Mondal, D. Borah, R. Mazumdar and B. Mondal, *Inorg. Chem.*, 2019, **58**, 14701; (*e*) R. Mazumdar, B. Mondal, S. Saha, B. Samanta and B. Mondal, *J. Inorg. Biochem.*, 2022, **228**, 111698.
17 K. Fujisawa, S. Chiba, Y. Miyashita and K. Okamoto, *Eur. J. Inorg. Chem.*, 2009, **48**, 3921.
18 (*a*) C. R. Randall, Y. Zang, A. E. True, L. Que Jr., J. M. Charnock, C. D. Garner, Y. Fujishima, C. J. Schofield and J. E. Baldwin, *Biochemistry*, 1993, **32**, 6664; (*b*) C. R. Randall, L. Shu, Y.-M. Chiou, K. S. Hagen, M. Ito, N. Kitajima, R. J. Lachicotte, Y. Zang and L. Que Jr., *Inorg. Chem.*, 1995, **34**, 1036.
19 (*a*) Y.-M. Chiou and L. Que Jr., *Inorg. Chem.*, 1995, **34**, 3270; (*b*) H. T. Dong, A. L. Speelman, C. E. Kozemchak, D. Sil, C. Krebs and N. Lehnert, *Angew. Chem., Int. Ed.*, 2019, **58**, 17695.
20 M. Ray, A. P. Golombek, M. P. Hendrich, G. P. A. Yap, L. M. Liable-Sands, A. L. Rheingold and A. S. Borovik, *Inorg. Chem.*, 1999, **38**, 3110.
21 B. Mondal, S. Saha, D. Borah, R. Mazumdar and B. Mondal, *Inorg. Chem.*, 2019, **58**, 1234.
22 R. D. Jones, D. A. Summerville and F. Basolo, *Chem. Rev.*, 1979, **79**, 139.
23 M. Suzuki, T. Ishiguro, M. Kozuka and K. Nakamoto, *Inorg. Chem.*, 1981, **20**, 1993.
24 (*a*) O. A. Ileperuma and R. D. Feltham, *Inorg. Chem.*, 1977, **16**, 1876; (*b*) A. L. Speelman, B. Zhang, C. Krebs and N. Lehnert, *Angew. Chem., Int. Ed.*, 2016, **55**, 6685.
25 R. Flammang, M. Barbieux-Flammang, Y. V. Haverbeke, A. Luna and J. Tortajada, *J. Phys. Org. Chem.*, 2000, **13**, 13.
26 H. Sugimoto and D. T. Sawyer, *J. Am. Chem. Soc.*, 1985, **107**, 5712.
27 SMART, *SAINT and XPREP*, Siemens Analytical X-ray Instruments Inc., Madison, Wisconsin, USA, 1995.
28 G. M. Sheldrick, *SADABS: software for Empirical Absorption Correction*, University of Gottingen, Institut fur Anorganische Chemieder Universitat, Tammanstrasse 4, D-3400 Gottingen, Germany, 1999.
29 G. M. Sheldrick, *SHELXS*, University of Gottingen, Germany, 2016.
30 L. J. Farrugia, ORTEP-3 for Windows - a version of ORTEP-III with a Graphical User Interface (GUI), *J. Appl. Crystallogr.*, 1997, **30**, 565.